Available online at www.sciencedirect.com

SCIENCE DIRECT®

Journal of Organometallic Chemistry 689 (2004) 3513–3519

Journal of Organo metallic Chemistry

www.elsevier.com/locate/jorganchem

Carbon–carbon coupling on tetrahedral iridium clusters: X-ray molecular structures and multinuclear NMR studies of the two isomeric forms of $[Ir_4(CO)_6(\mu_3\text{-}\eta^2\text{-}HCCPh)(\mu_2\text{-}\eta^4\text{-}C_4H_2Ph_2)(\mu\text{-}PPh_2)_2]$

Maria Helena Araujo [a,1], Maria D. Vargas [a,*,2], Anthony G. Avent [b], Dario Braga [c], Fabrizia Grepioni [c,*]

[a] *Instituto de Química, Universidade Estadual de Campinas, CP 6154, Campinas, 13081-970, SP, Brazil*
[b] *Chemistry Department, University of Sussex, Brighton, BN1 9QJ, UK*
[c] *Dipartimento di Chimica "G.Ciamician", Universitá degli Studi di Bologna, Via Selmi 2, 40126, Bologna, Italy*

Received 14 July 2004; accepted 3 August 2004
Available online 11 September 2004

Abstract

The reactions of $[HIr_4(CO)_9(Ph_2PC{\equiv}CPh)(\mu\text{-}PPh_2)]$ (**1**) or $[Ir_4(CO)_8(\mu_3\text{-}\eta^2\text{-}HCCPh)(\mu\text{-}PPh_2)_2]$ (**2**) with $HC{\equiv}CPh$ gave two isomeric forms of $[Ir_4(CO)_6(\mu_3\text{-}\eta^2\text{-}HCCPh)(\mu_2\text{-}\eta^4\text{-}C_4H_2Ph_2)(\mu\text{-}PPh_2)_2]$ (**3** and **4**) in good yields as the only products. These compounds were characterized with analytical and spectroscopic data including ^1H, ^{13}C and ^{31}P NMR (1 and 2D) spectroscopy and their molecular structures were established by X-ray diffraction studies. Compounds **3** and **4** exhibit the same distorted butterfly metal polyhedral arrangement of metal atoms with two μ-PPh_2 that occupy different positions in the structures of the two isomers. Both molecules contain a HCCPh ligand bonded in a $\mu_3\text{-}\eta^2\text{-}//$ mode to one of the wings of the butterfly and a metallacyclic ring, which resulted from head-to-tail coupling, in the case of $[Ir_4(CO)_6(\mu_3\text{-}\eta^2\text{-}HCCPh)\{\mu_2\text{-}\eta^4\text{-}(H)CC(Ph)C(H)C(Ph)\}(\mu\text{-}PPh_2)_2]$ (**3**) and tail-to-tail coupling, in that of $[Ir_4(CO)_6(\mu_3\text{-}\eta^2\text{-}HCCPh)\{\mu_2\text{-}\eta^4\text{-}(H)CC(Ph)C(Ph)C(H)\}(\mu\text{-}PPh_2)_2]$ (**4**), and which is linked to two metal atoms of the second wing of the butterfly.

Keywords: Tetrairidium cluster; Alkyne; C–C coupling; X-ray molecular structure

1. Introduction

The reactions of alkynes with metal carbonyl clusters have received considerable attention in the last 20 years or so. Systematic studies involving the modes of interaction of alkynes [1–6], activation of C–C [7,8] and C–H [9,10] bonds, cyclotrimerization [10], oligomerization [11–14] and coupling with other ligands such as acetylides and phosphinoalkynes [15–17], incorporation of CO [16] and insertion into M–P bonds [18,19] have been performed and several reaction pathways elucidated, especially those involving clusters of the iron triad [2,20,21]. In contrast, reports on the reactions of iridium clusters with alkynes are rare, most probably due to the lack of suitably reactive starting materials besides $[Ir_4(CO)_{12}]$ and $[Ir_6(CO)_{16}]$. The only reports in the literature involving iridium clusters describe the reactions of

---

[*] Corresponding authors. Tel.: +55 21 22660167; fax: +55 21 27178375.

E-mail addresses: mharaujo@ufmg.br (M. Helena Araujo), mdvargas@vm.uff.br (M.D. Vargas).

[1] Present address: Departamento de Química, ICEx, Universidade Federal de Minas Gerais, Belo Horizonte MG, 31270-901, Brazil.

[2] Instituto de Química, Universidade Federal Fluminense, Outeiro de São João Batista s/n, Campus do Valonguinho, Centro, Niterói, RJ 24.020-150, Brazil.

0022-328X/$ - see front matter © 2004 Elsevier B.V. All rights reserved.
doi:10.1016/j.jorganchem.2004.08.010

this tetranuclear cluster under thermolytic conditions with $C_2(COOMe)_2$, to yield $[Ir_4(CO)_8\{C_2(COOMe)_2\}_4]$ [22], and with cod (cod = cyclooctadiene), to give the alkyne containing clusters $[Ir_4(CO)_5(cod)_2(C_8H_{10})]$ and $[Ir_7\text{-}(CO)_{12}(cod)(C_8H_{11})(C_8H_{10})]$ [23,24] all in very low yields, and that of the oxidation of $[Ir_6(CO)_{15}]^{2-}$ with ferrocinium in the presence of PhCCPh to yield $[Ir_6\text{-}(CO)_{14}(\mu_3\text{-}\eta^2\text{-}HCCPh)]$ and $[Ir_6(CO)_{12}(\mu_3\text{-}\eta^2\text{-}HCCPh)_2]$ [25]. The cluster $[HIr_4(CO)_{10}(\mu\text{-}PPh_2)]$ [26] has proven itself a good entry into tetranuclear iridium organometallic chemistry [27–35]. Its derivative $[HIr_4\text{-}(CO)_9(Ph_2PC\equiv CPh)(\mu\text{-}PPh_2)]$ (**1**) undergoes a selective rearrangement under mild conditions to give $[Ir_4\text{-}(CO)_8(\mu_3\text{-}\eta^2\text{-}HCCPh)(\mu\text{-}PPh_2)_2]$ (**2**) [34]. The process was envisaged as proceeding by formation of a reactive intermediate containing phosphido and acetylide ligands, followed by migration of the hydride onto the α-carbon to yield the $\mu_3\text{-}\eta^2\text{-}HCCPh$ ligand. Studies of the reactivity of ruthenium dimers and trinuclear clusters containing $\mu_2\text{-}\eta^2$- and $\mu_3\text{-}\eta^2$-coordinated acetylides, respectively, have evidenced that these ligands are electron deficient and therefore susceptible to nucleophilic attack [2,5]. This work describes our attempts at trapping the possible acetylide containing intermediate by investigating the rearrangement of **1** in the presence of $HC\equiv CPh$. Two isomeric forms of $[Ir_4(CO)_6(\mu_3\text{-}\eta^2\text{-}HCCPh)(\mu_2\text{-}\eta^4\text{-}C_4H_2Ph_2)(\mu\text{-}PPh_2)_2]$ (**3**) and (**4**) were obtained in high yields, as the result of head-to-tail and tail-to-tail couplings of two $HC\equiv CPh$ molecules, respectively.

2. Results and discussion

2.1. Reactions of $[HIr_4(CO)_9(Ph_2PC\equiv CPh)(\mu\text{-}PPh_2)]$ (1) and $[Ir_4(CO)_8(\mu_3\text{-}\eta^2\text{-}HCCPh)(\mu\text{-}PPh_2)_2]$ (2) with $HC\equiv CPh$

The reaction of $[HIr_4(CO)_9(Ph_2PC\equiv CPh)(\mu\text{-}PPh_2)]$ (**1**) with $HC\equiv CPh$ was investigated under various conditions. When carried out at 25 °C for 24 h or at 40 °C for 4 h, in toluene or in CH_2Cl_2, with one equiv. of $HC\equiv CPh$, formation of $[Ir_4(CO)_8(\mu_3\text{-}\eta^2\text{-}HCCPh)(\mu\text{-}PPh_2)_2]$ (**2**) exclusively was observed, as the result of the decarbonylation and rearrangement of **1** [27]. When the reaction mixture was heated at 80 °C in toluene for 4 h with two equiv. of $HC\equiv CPh$, however, two novel red compounds $[Ir_4(CO)_6(\mu_3\text{-}\eta^2\text{-}HCCPh)\{\mu_2\text{-}\eta^4\text{-}(H)CC(Ph)C(H)C(Ph)\}(\mu\text{-}PPh_2)_2]$ (**3**) and $[Ir_4(CO)_6(\mu_3\text{-}\eta^2\text{-}HCCPh)\{\mu_2\text{-}\eta^4\text{-}(H)\text{-}CC(Ph)C(Ph)C(H)\}(\mu\text{-}PPh_2)_2]$ (**4**) were isolated in about 35% and 30% yields, respectively, after TLC.

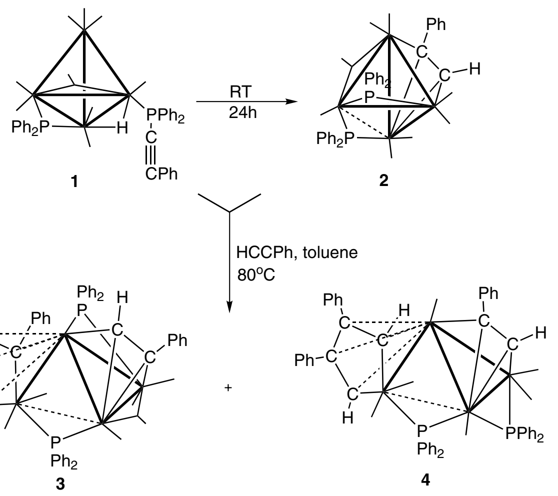

Scheme 1.

As illustrated in Scheme 1, the two isomeric complexes contain an iridiumcyclopentadiene moiety formally resulting from the coupling of two phenylacetylene molecules, and a "lone" HCCPh ligand coordinated to a triangular face. In an attempt to isolate complexes less substituted, this reaction was carried out with one equiv. of $HC\equiv CPh$, but again compounds **3** and **4** were obtained, albeit in lower yields, besides compound **2** and unreacted **1**. In order to check whether compounds **3** and **4** were formed from **1** or from **2**, the reaction of cluster **2** with $HC\equiv CPh$ was also investigated (toluene, 80 °C for 12 h). A longer reaction time was necessary to yield compounds **3** and **4**, which were isolated in 45% and 35% yields, respectively, i.e. in better yields than from **1**, in addition to unreacted **2**. Also in this case best yields of the products were obtained with two equiv. of $HC\equiv CPh$.

Compounds **3** and **4** were initially formulated on the basis of spectroscopic and analytical data, which were not sufficient to proposed unambiguous structures for the two isomers. X-ray diffraction studies, therefore, had to be carried out on both compounds and are discussed below, followed by that of the NMR data.

*2.2. X-ray diffraction studies of **3** and **4***

The molecular structures of compounds **3** and **4** and the atomic labeling schemes are shown in Figs. 1 and 2, respectively. Selected bond lengths and angles are shown in Table 1. The molecular structures of the two compounds are very similar and therefore will be described together. Both exhibit a distorted butterfly arrangement of iridium atoms [angles between Ir(1)–Ir(2)–Ir(4) and Ir(1)–Ir(2)–Ir(3) planes 54.244(17)° and 60.834(19)°, **3** and 56.212(14)° and 59.000(14)°, **4**] with one elongated wing edge [Ir(2)–Ir(4) 3.1945(8), **3** and 3.0173(6) Å, **4**] bridged by a PPh_2 group [Ir(2)–P(2)–Ir(4) 86.44(12), **3** and 80.91(8)°, (**4**)]. The second bridging PPh_2 ligand occupies two different edges of the same wing in the two clusters: in **3** it spans the Ir(1)–Ir(3) edge [2.7919(7) Å] whereas in **4**, it bridges the unusually short Ir(2)–Ir(3) edge [2.6658(5) Å]. In fact the shortest distance observed so far between iridium atoms spanned

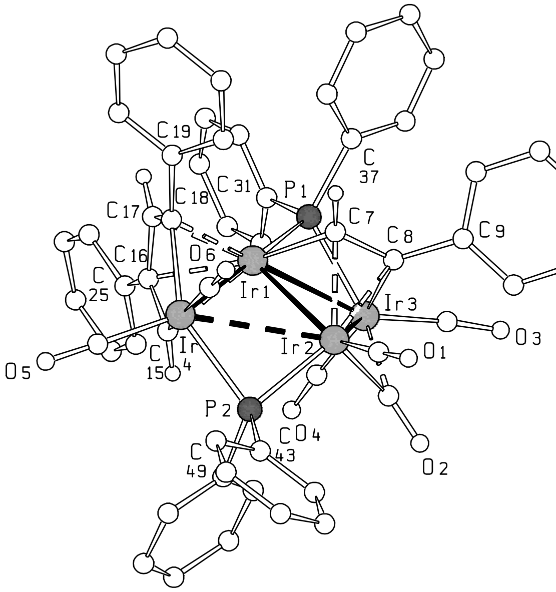

Fig. 1. Molecular structure of [$Ir_4(CO)_6(\mu_3$-η^2-HCCPh){μ_2-η^4-(H)CC(Ph)C(H)C(Ph)}(μ-$PPh_2)_2$] (**3**).

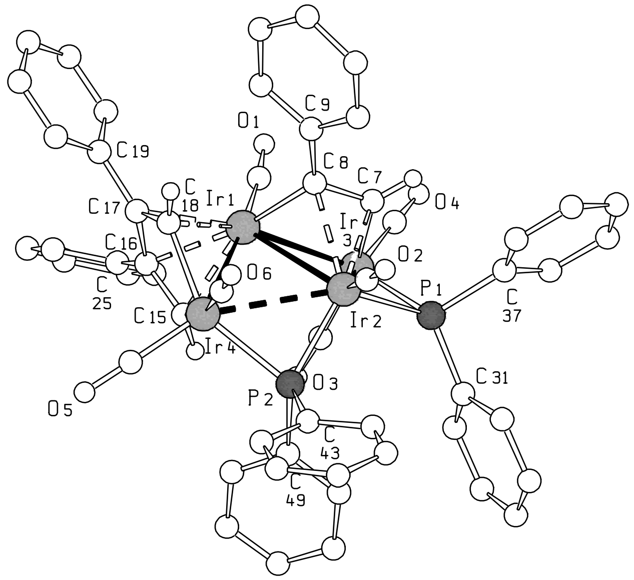

Fig. 2. Molecular structure of [$Ir_4(CO)_6(\mu_3$-η^2-HCCPh){μ_2-η^4-(H)CC(Ph)C(Ph)C(H)}(μ-$PPh_2)_2$] (**4**).

Table 1
Selected intramolecular distances (Å) and angles (°) for compounds **3** and **4**

Distances (Å)	3	4
Ir(1)–Ir(2)	2.7290(7)	2.9132(5)
Ir(1)–Ir(3)	2.7919(7)	2.7558(6)
Ir(1)–Ir(4)	2.7320(7)	2.7954(6)
Ir(2)–Ir(3)	2.7846(7)	2.6658(6)
Ir(2)–Ir(4)	3.1945(8)	3.0173(6)
Ir(1)–P(1)	2.243(4)	**
Ir(2)–P(1)	**	2.291(3)
Ir(3)–P(1)	2.353(4)	2.294(3)
Ir(2)–P(2)	2.300(4)	2.315(3)
Ir(4)–P(2)	2.365(4)	2.335(3)
Ir(1)–C(7)	2.031(13)	**
Ir(1)–C(8)	**	2.033(9)
Ir(2)–C(7)	2.226(12)	2.234(9)
Ir(2)–C(8)	2.266(13)	2.362(8)
Ir(3)–C(7)	**	2.067(9)
Ir(3)–C(8)	2.076(12)	**
Ir(1)–C(15)	2.223(12)	2.213(9)
Ir(1)–C(16)	2.280(12)	2.224(10)
Ir(1)–C(17)	2.206(13)	2.269(9)
Ir(1)–C(18)	2.205(13)	2.228(9)
Ir(4)–C(15)	2.051(14)	2.066(9)
Ir(4)–C(18)	2.096(13)	2.092(9)
C(7)–C(8)	1.422(18)	1.393(12)
C(8)–C(9)	1.520(13)	1.476(10)
C(15)–C(16)	1.396(18)	1.422(12)
C(16)–C(17)	1.422(17)	1.456(13)
C(17)–C(18)	1.402(18)	1.408(12)
C(16)–C(25)	1.517(13)	1.487(10)
Ir(2)–P(2)–Ir(4)	86.44(12)	80.91(8)
Ir(1)–P(1)–Ir(3)	74.76(10)	**
Ir(2)–P(1)–Ir(3)	**	71.09(8)
C(7)–C(8)–C(9)	123.0(11)	122.3(8)
C(17)–C(18)–C(19)	118.2(11)	**
C(15)–C(16)–C(17)	111.5(11)	113.7(8)
C(16)–C(17)–C(19)	**	128.7(8)
C(16)–C(17)–C(18)	115.9(12)	113.0(8)
C(15)–C(16)–C(25)	**	124.0(8)
Ir(2)–C(2)–O(2)	141.4(14)	**
Ir(3)–C(2)–O(2)	136.0(13)	**
Dihedral angles	154° (butterfly)	141° (butterfly)

by a μ-PPh_2 group is 2.792(2) Å in [$HIr_4(CO)_{10}$-(PPh_2)] [26]. Whereas compound **3** contains a bridging CO ligand spanning the Ir(2)–Ir(3) edge, two terminal CO's bonded to Ir(3) and Ir(4) and one to Ir(2), in compound **4** all six CO ligands are terminally bonded, one to Ir(1) and Ir(2) and two to Ir(3) and Ir(4).

Both molecules contain a μ_2-η^4-$C_4H_2Ph_2$ ligand, formed as a result of head-to-tail, **3**, and tail-to-tail, **4**, condensation of two PhCCH molecules. This ligand is bonded in a σ-fashion to Ir(4) to form a metallacyclopentadiene [Ir(4)–C(15) 2.051(14), **3**, 2.066(9) Å, **4** and Ir(4)–C(18) 2.096(13), **3**, 2.092(9) Å, **4**] that π-interacts with Ir(1) via all its carbon atoms as in the well known ferroles or ferracyclopentadiene complexes [36] and other dimers [37,38] and cluster compounds [39]. As such these ligands act formally as 6 electron donors. The Ir(4)–Cσ-bond distances are within values observed for σ-Ir-sp^2C bond lengths in other clusters, e.g. [$Ir_4(CO)_8(\mu_3$-η^3-$Ph_2PC(H)CPh)(\mu$-$PPh_2)(PCy_3)$] [2.07(1) Å] [27] and [$HIr_4(CO)_7(PPh_3)(\mu_3$-η^2-PhPCPh=CPh)(μ-PPh_2)] [2.17(3) Å] [33]. In **3**, the C–C bond distances of the metallacyclodiene show a more localized pattern [C(15)–C(16) 1.396(18), C(16)–C(17) 1.422(17), C(17)–C(18) 1.402(18) Å] than in **4** [C(15)–C(16) 1.422(12), C(16)–C(17) 1.456(13), C(17)–C(18) 1.408(12) Å], but the average C–Ir(1) distances [2.2285(12), **3** and 2.2335(9) Å, **4**] are similar in the two molecules. The Ir(1)–Ir(4) distances [2.7320(7), **3** and 2.7954(6) Å, **4**] in the two molecules are within average values observed in Ir_4 clusters.

In the two compounds the HCCPh ligand is bonded in the commonly encountered [2] μ_3-η^2-fashion, // to the Ir(1)–Ir(2)–Ir(3) butterfly wing, but with different orientations: in **4**, the Ph substituent is directed towards the hinge of the butterfly, and in **3**, towards the wing end. In both compounds the alkyne ligand formally contributes 4 electrons to the cluster via two σ interactions with Ir(1) and Ir(3) [C(7)–Ir(1) 2.031(13), C(8)–Ir(3) 2.076(12) Å, **3** and C(7)–Ir(3) 2.067(9) and C(8)–Ir(1) 2.033(9) Å], **4**, and one π interaction with Ir(2) [C(7)–Ir(2) 2.226(12), **3**, 2.234(9) Å, **4**, and C(8)–Ir(2) 2.266(13), **3**, and 2.362(8) Å, **4**]. The C(7)–C(8) distances observed in the two compounds [1.422(18), **3**, and 1.393(12) Å], **4** are shorter than in $[Ir_4(CO)_8(\mu_3\text{-}\eta^2\text{-}HCCPh)(\mu_2\text{-}PPh_2)_2]$ [1.51(6) Å], but within the values encountered in other Ir clusters, e.g. $[Ir_6(CO)_{12}(\mu_3\text{-}\eta^2\text{-}HCCPh)_2]$ [1.39(2) Å] [25] and ruthenium clusters which contain the alkyne bonded in the same fashion (1.33 1.45 Å) [2]. In both compounds the C(7)–C(8)–C(9) angles [123.0(11), **3**, and 122.3(8)°, **4**, are typical of sp^2-hybridized carbons.

The structures of compounds **3** and **4** are reminiscent of that of $[Os_3(\mu_3\text{-}\eta^2\text{-}PhCCPh)(\mu_2\text{-}\eta^4\text{-}C_4Ph_4)(CO)_7]$ [39] a low yield product of the reaction of $[Os_3(CO)_{12}]$ with PhCCPh, under thermolytic conditions. Possible intermediates in the formation of this species were also characterized by X-ray analyses, viz. $[Os_3(\mu_3\text{-}\eta^2\text{-}//PhCCPh)(CO)_{10}]$, $[Os_3(\mu_2\text{-}\eta^4\text{-}C_4Ph_4)(CO)_9]$ and $[Os_3(\mu_2\text{-}\eta^4\text{-}C_4Ph_4)(CO)_8]$ [40–42], thus suggesting that metallacycle formation precedes interaction of the third acetylene molecule.

2.3. Solution characterization of compounds 3 and 4

The solution structures of compounds **3** and **4** are in agreement with the structures determined in the solid state. A detailed investigation of the structure of compound **3** was undertaken by 1D, 2D and VT NMR experiments (see Section 4 and structure below).

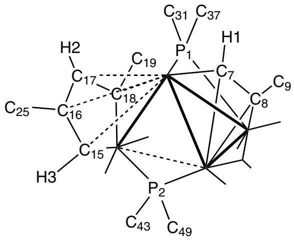

3

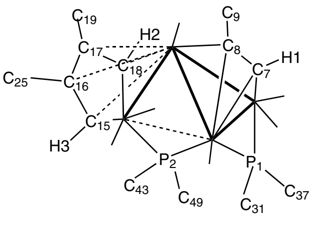

4

The room temperature ^1H NMR spectrum of this compound, in CD_2Cl_2, exhibited two resonances at δ 9.25 (s) and 5.37 (dd, $J_{H\text{–}P}$ 9.7, $J_{H\text{–}H}$ 2.5 Hz), attributed to the CH aliphatic groups, besides resonances due to the aromatic protons. The third aliphatic proton was evidenced by NOE intensity enhancement experiments involving nearby protons, which allowed the assignment of the majority of the protons in this cluster. Only assignments of the aliphatic protons will be discussed below. With irradiation at δ 9.25 it was possible to assign this resonance to H-1, because NOE intensity enhancements of 6.7% in the doublet at δ 6.57 (*ortho*-H, C-9), of 5.7% in the doublet at δ 7.43 (*ortho*-H, C-19), of 2.1% in the δ 7.33–7.21 multiplet (*ortho*-H, C-31) and of 2.0% in the multiplet at δ 8.02–7.98 (*ortho*-H, C-43) were observed. The assignments of the resonance at δ 5.37 to H-3 and of the hidden signal under the phenyl protons at δ 7.26, to H-2, were only possible after irradiation of the doublet at δ 6.61 (*ortho*-H, C-25) which gave a 13.3% NOE for the δ 5.37 (dd, H-3) resonance and a 11.6% NOE for the δ 7.26 (m, H-2) signal. Similarly, irradiation of the multiplet at δ 6.78–6.72 (*ortho*-H C-37, *meta*-H, C-37 and *meta*-H, C-25) gave a 9.0% NOE intensity enhancement for the doublet at δ 6.61 (*ortho*-H, C-25) and a 3.0% NOE measured for the multiplet at δ 7.26 (H-2). Selective decoupling at δ 7.26 resulted in the removal of the smallest coupling $J_{H3\text{–}H2}$ 2.5 Hz from the signal at δ 5.37 establishing unambiguously the coupling between H-3 and H-2. The resonances at δ 9.25 (H-1) and δ 5.37 (H-3) in the ^1H NMR spectrum obtained at 303 K showed ^{13}C satellites of 162 Hz, typical of sp^2 hybridized carbons.

The room temperature ^1H NMR spectrum of compound **4**, in $CDCl_3$, exhibited, besides the resonances due to the phenyl protons, two doublets at δ 5.73 (d, $J_{H\text{–}P}$ 6.0 Hz) and 6.61 (d, $J_{H\text{–}P}$ 6.8 Hz), attributed to the CH aliphatic groups. The third aliphatic proton was hidden under the aromatic groups and was identified in the HSQC 2D NMR spectrum. The CH groups in compounds **3** and **4** were assigned by a DEPT-90 experiment. The identification of the three aliphatic carbons, in **3** and **4**, and the correlation between the ^1H chemical shifts were achieved by an HSQC 2D NMR experiment. In compound **3**, the peak at δ 119.86 was attributed to the alkyne C-7, which is correlated with H-1 at δ 9.25, whereas those at δ 93.52 and 102.20 which correlated with H-2 and H-3 were assigned to the metallacyclo C-17 and C-15, respectively. In compound **4**, the peak at δ 116.00 is correlated to the proton at δ 5.73 (d), whereas those at δ 108.00 and at δ 90.00 are correlated to δ 7.80 (m) and δ 6.61 (d), respectively. In the room temperature $^{31}P\{^1H\}$ NMR spectra of compounds **3** (in CD_2Cl_2) and **4** (in $CDCl_3$) the low frequency resonance [δ 36.20 (br) and 77.36 (d, $J_{P1\text{–}P2}$ 12.9 Hz), respectively] was assigned to P2 which spans the same iridium atoms that do not interact [Ir(2)–Ir(4) 3.1945(8) and 3.0173(6) Å, respectively]. The resonance attributed to P1 appears at much higher frequency in compound **4**, at δ 252.20 (d), than in compound **3**, at δ 194.50 (d,

J_{P1-P2} 11.0 Hz), reflecting the shorter P1 bridged Ir(2)–Ir(3) distance [2.6658 (6) Å] in **4**, in comparison to the P1 bridged Ir(1)–Ir(3) distance [2.7919(7) Å] in the molecular structure of compound **3**. The dependence of the δ ^{31}P for phosphido bridges on metal–metal interactions is well established [43]. Systematic correlations between the upfield ^{31}P chemical shifts for the phosphido bridges and the increase in the Ir–Ir distances and Ir–P–Ir angles have been found for various derivatives of [$HIr_4(CO)_{10}(\mu\text{-}PPh_2)$] [26,33,44].

2.4. Speculations on the mechanism of formation of ***3*** *and* ***4***

We have no hints about the pathways of formation of compounds **3** and **4**, as no intermediate was spotted upon monitoring the reaction by TLC and ^{31}P NMR spectroscopy. Nonetheless, based on our results and on work by Sappa et al. [16] on the reactions of [$HRu_3(CO)_8(MeCN)(\mu_3\text{-}\eta^2\text{-}C_2{}^tBu)$] with HC≡C^{t}Bu, a qualitative discussion on the formation of **3** and **4** is attempted below.

The impossibility to isolate intermediate compounds resulting from the incorporation of only one HC≡CPh suggests that the generation of a vacant coordination site for the activation of the first alkyne, via CO dissociation or Ir–Ir bond cleavage, is extremely slow, whereas the subsequent processes leading to the formation of **3** and **4**, including activation of the second alkyne are fast. Indeed, the activated ruthenium cluster, which looses easily the MeCN ligand, reacts at room temperature with excess HC≡C^{t}Bu to give a product in which three alkyne molecules were incorporated, as the result of C–C, C–O and C–Ru bonds formation [16].

For the reaction between **1** and HC≡CPh it is reasonable to suggest a first step involving intramolecular oxidative addition of the Ph_2PCCPh P–C bond, since this is a low energy process, which occurs at 42 °C (and leads to the formation of **2**). At 80 °C, however, compound **2** is not detected upon monitoring the reaction, in spite of the fact that the reaction of **2** with HC≡CPh under the same conditions is markedly slower. The acetylide containing intermediate would therefore undergo rapid nucleophilic attack of HC≡CPh (instead of insertion into the Ir–H bond), with acetylide–alkyne condensation, to give head-to-tail or tail-to-tail coupling products in approximate equal amounts; insertion into the Ir–H bond would then lead to the formation of the $IrC_4H_2Ph_2$ metallacycles.

To account for the fact that same product distribution is obtained from the analogous reaction of **2**, an equilibrium involving oxidative addition/reductive elimination of the coordinated HCCPh to yield a hydrido-acetylido species is proposed. Although shifted in the direction of the reductive elimination process (this would account for the slow reaction of **2**), nucleophilic attack of HC≡CPh, as described above, would drive the equilibrium towards formation the oxidative addition product. Thereafter, similar pathways would be followed in both reactions for the incorporation of the second HC≡CPh molecule.

3. Conclusions

Considering the complexity of both starting materials **1** and **2** and products **3** and **4**, and the number of alternative reaction pathways available for phosphide clusters containing terminal alkynes, under thermolytic conditions, e.g., C–H, P–Ph and C=O bonds activation, P–C and C–C bonds formation, CO incorporation in the organic chains and cluster breakdown, the selectivity observed is impressive indeed. This selectivity might be associated to the fact that the average oxidation state of the iridium atoms in **2** and in the presumed compound, formed after P–C bond cleavage in **1**, is +1, i.e. further oxidative additions might be unfavorable.

4. Experimental

4.1. General procedures

All manipulations and reactions were carried out under dry argon, unless otherwise specified, using standard Schlenk techniques. CH_2Cl_2 was dried over CaH_2, hexane and toluene over sodium. Solvents were freshly distilled under argon and freed from dissolved oxygen, where compatible, by freeze degassing before use. HC≡CPh (Aldrich) was distilled before use, and [$HIr_4(CO)_{10}(\mu\text{-}PPh_2)$] [26], [$HIr_4(CO)_9(Ph_2PC{\equiv}CPh)(\mu\text{-}PPh_2)$] (**1**) [34] and [$Ir_4(CO)_8(\mu_3\text{-}\eta^2\text{-}HCCPh)(\mu\text{-}PPh_2)_2$] (**2**) [34] were prepared by literature methods.

The progress of the reactions was monitored by analytical TLC (pre-coated plates, silica gel F 254, 0.25 mm thick; Merck) and IR spectroscopy. The separation and purification of the reaction products were carried out in air by preparative TLC (2 mm thick glass-backed silica plates, 20 × 20 cm, prepared from silica gel GF 254, Fluka) and the compounds were extracted from silica with CH_2Cl_2.

Infrared spectra were recorded on a Bomen (FT-IR Michelson) spectrophotometer scanning between 2200 and 1600 cm^{-1} (ν_{CO}) using CaF_2 liquid cells. Microanalyses were performed on a Perkin–Elmer 2401 Elemental Analysis Instrument. Solution NMR spectra were recorded on a Varian Inova-500, Bruker AMX 500, AC 300P or AC 200 spectrometers. Signals were attributed based on the following NMR experiments: ^{1}H, ^{13}C, ^{31}P, NOE, 2D COSY, 2D HSQC, standard pulse sequences were used for the experiments. Hydrogen, carbon and phosphorus atoms are labeled as in the crystal structures. The phenyl groups are identified by the first quaternary carbon bonded to the phosphorus of the phosphido groups or to the carbons of the organic chains and labeled as in the crystal structure. Deuterated solvents were used as locks and references: ^{1}H relative to the proton resonance resulting from incomplete deuteration of the $CDCl_3$ (δ 7.27), C_6D_6 (δ 7.16) or CD_2Cl_2 (δ 5.32); ^{13}C relative to the carbon of the $CDCl_3$ (δ 77.23) or CD_2Cl_2 (δ 54.00) and for ^{31}P, external 85% H_3PO_4.

4.2. *Preparation of* $[Ir_4(CO)_6(\mu_3\text{-}\eta^2\text{-}HCCPh)\{\mu_2\text{-}\eta^4\text{-}(H)CC(Ph)C(H)C(Ph)\}(\mu\text{-}PPh_2)_2]$ *(**3**) and* $[Ir_4(CO)_6(\mu_3\text{-}\eta^2\text{-}HCCPh)\{\mu_2\text{-}\eta^4\text{-}(H)CC(Ph)C(Ph)C(H)\}(\mu\text{-}PPh_2)_2]$ *(**4**)*

4.2.1. *Method 1*

To a dark orange solution of **1** (100 mg, 0.07 mmol), in toluene (15 mL), HC≡CPh (18.0 μL, 0.14 mmol) was added. The mixture was heated at 80 °C for 4 h, after which time the solvent was evaporated in vacuo and the mixture was dissolved in CH_2Cl_2 (2 mL). Purification by preparative TLC (ethyl acetate/hexane, 1:6.3 as eluent) afforded the two red compounds **3** (R_f 0.54, 36 mg, 35%) and **4** (R_f 0.47, 30 mg, 30%) and five other species in minute amounts, according to the $^{31}P\{^{1}H\}$ NMR spectrum, which were not further characterized. Anal. Calcd. for $C_{42}H_{28}O_6P_2Ir_4$: C, 34.5; H, 1.9. Found: C, 34.7; H, 2.1. IR ν_{CO} (hexane) for **3**: 2077 w, 2053 s, 2041 vs, 2014 s, 1996 vs, 1974 m, 1818 m, cm^{-1}; NMR (CD_2Cl_2, 25 °C): ^{1}H (500 MHz), δ 5.37 (dd, $J_{H3–H2}$ 2.5 Hz and $J_{P2–H3}$ 9.7 Hz, 1CH 3), 7.26 (m, 1CH 2), 9.25 (s, 1CH 1), 8.02–7.98 (m, 2 H, *ortho*-H C43), 7.80–7.76 (m, 2 H, *ortho*-H, C49), 7.43 (d, $J_{H–H}$ 1.4 Hz, 2 H, *ortho*-H, C19), 7.33–7.27 (m, 2 H, *ortho*-H, C31), 6.78–6.72 (m, 2 H, *ortho*-H C37), 6.61 (d, $J_{H–H}$ 1.2 Hz, 2 H, *ortho*-H, C25), 6.57 (d, $J_{H–H}$ 1.4 Hz, 2 H, *ortho*-H, C9); $^{13}C\{^{1}H\}$ (125.69 MHz), δ 115.61 (d, $J_{C–P}$ 7.0 Hz, $C_{quat.}$ Ph), 130.14 (s, $C_{quat.}$ Ph), 132.90 (d, $J_{C–P}$ 48.9 Hz, $C_{quat.}$ Ph), 134.86 (s, $C_{quat.}$ Ph), 136.35 (d, $J_{C–P}$ 36.9 Hz, $C_{quat.}$ Ph), 137.76 (s, $C_{quat.}$ Ph), 138.90 (d, $J_{C–P}$ 32.3 Hz, $C_{quat.}$ Ph), 145.77 (d, $J_{C–P}$ 25.5 Hz, $C_{quat.}$ Ph), 129.45 (d, $J_{C–P}$ 11.5 Hz, *C*H, Ph), 129.16 (d, $J_{C–P}$ 9.2 Hz, *C*H, Ph), 128.94 (d, $J_{C–P}$ 11.0 Hz, *C*H, Ph), 126.86 (d, $J_{C–P}$ 9.3 Hz, *C*H, Ph), 125.79 (d, $J_{C–P}$ 2.1 Hz, *C*H, Ph), 125.49 (d, $J_{C–P}$ 2.0 Hz, *C*H, Ph), 125.36 (s, *C*H, Ph), 125.16 (s, *C*H, Ph), 124.56–124.42 (m, *C*H, Ph), 124.36 (s, *C*H, Ph), 124.21 (s, *C*H, Ph), 124.12 (d, $J_{C–P}$ 10.2 Hz, *C*H, Ph), 123.87 (d, $J_{C–P}$ 10.4 Hz, *C*H, Ph), 123.57 (s, *C*H, Ph), 123.21 (d, $J_{C–P}$ 2.2 Hz, *C*H, Ph), 122.74 (s, *C*H, Ph), 122.54 (s, *C*H, Ph), 122.40 (s, *C*H, Ph), 119.86 (s, *C*H), 102.20 (d, $J_{C–P}$ 4.8 Hz, *C*H), 93.52 (s, *C*H); $^{31}P\{^{1}H\}$ (121.49 MHz), δ 194.50 (d, $J_{P–P}$ 11.0 Hz) and 36.20 (br, s). IR ν_{CO} (hexane) for **4**: 2064 m, 2047 vs, 2037 s, 2018 s, 2007 s, 1998 s, 1975 m, cm^{-1}; NMR ($CDCl_3$, 25 °C): ^{1}H (500 MHz), δ 5.73 (d, $J_{P–H}$ 6.0 Hz, CH), 6.61 (d, $J_{P–H}$ 6.8 Hz, CH), 7.80 (br, s, CH), 8.00–6.62 (m, Ph); ^{13}C (125.69 MHz), δ 124.0 ($C_{quat.}$ Ph), 131.32 ($C_{quat.}$ Ph), 137.96 (d, $J_{C–P}$ 9.3 Hz, *C*H, Ph), 134.98 (d, $J_{C–P}$ 10.8 Hz, *C*H, Ph), 132.67 (d, $J_{C–P}$ 11.7 Hz, *C*H, Ph), 132.42 (s, *C*H, Ph), 130.88 (s, *C*H, Ph), 130.61 (s, *C*H, Ph), 129.91 (s, *C*H, Ph), 129.65 (s, *C*H, Ph), 128.78 (s, *C*H, Ph), 128.50–128.32 (m, *C*H, Ph), 127.86 (d, $J_{C–P}$ 11.7 Hz, *C*H, Ph), 127.37–127.23 (m, *C*H, Ph), 127.16 (s, *C*H, Ph), 126.89 (s, *C*H, Ph), 116.00 (s, *C*H), 108.00 (s, *C*H), 90.00 (s, *C*H); $^{31}P\{^{1}H\}$ (121.49 MHz), δ 252.20 (d, $J_{P–P}$ 13.0 Hz, μ-*P*Ph$_2$) and 77.36 (d).

4.2.2. *Method 2*

To an orange solution of **2** (100 mg, 0.07 mmol), in toluene (15 mL), HC≡CPh (18.0 μL, 0.14 mmol) was added. The mixture was heated at 80 °C for 12 h. The solvent was evaporated and the mixture was separated by TLC with ethyl acetate/hexane (1:6.3) to yield unreacted **2** (R_f 0.72, 10 mg, 10%), and the two red isomers **3** (46 mg, 45%) and **4** (36 mg, 35%).

4.3. *X-ray structural analysis of compounds **3** and **4***

The compounds were obtained as red crystals by slow diffusion of hexane in a very concentrated solution of the respective compound in CH_2Cl_2, at 25 ° C. Diffraction intensities were collected at 293 K on an Enraf-Nonius CAD-4 (compound **3**) or a Bruker Smart CCD (compound **4**) diffractometer equipped with a graphite monochromator (Mo Kα, $\lambda = 0.71069$ Å). Crystal data and details of measurements for compounds **3** and **4** are summarized in Table 2. Ψ-scan absorption correction was applied to compound **3** and SADABS to **4**. The computer program SHELXL97 [45] was used for structure solution and refinement. All non-H atoms

Table 2
Crystallographic data for compounds **3** and **4**

	3 · (0.5 CH_2Cl_2)	**4**
Formula	$C_{54.5}H_{39}ClIr_4O_6P_2$	$C_{54}H_{38}Ir_4O_6P_2$
M	1656.05	1613.58
Crystal system	Orthorhombic	Triclinic
Space group	$P2_1nb$	$P\bar{1}$
a (Å)	12.249(2)	12.4634(9)
b (Å)	19.753(2)	14.309(1)
c (Å)	22.050(3)	15.313(1)
α (°)	90	114.013(2)
β (°)	90	94.781(2)
γ (°)	90	91.569(2)
U (Å^3)	5335(1)	2480.3(3)
Z	4	2
D_c (g cm^{-3})	2.062	2.161
μ (mm^{-1})	10.102	10.810
Independent reflections	4862	14.408
R_1 (on F [$I > 2\sigma(I)$])	0.0272	0.0490
wR_2 (on F^2 all data)	0.0755	0.1007

(except for the dichloromethane solvent molecule in **3**) were refined anisotropically. H atoms bound to C atoms were added in calculated positions. The computer program SCHAKAL99 [46] was used for all graphical representations. Crystallographic data (excluding structure factors) for the structures reported in this paper have been deposited with the Cambridge Crystallographic Data Center as supplementary publication Nos. CCDC 243733 and CCDC 243734. Copies of the data can be obtained free of charge on application to CCDC, 12 Union Road, Cambridge CB2 1EZ, UK (fax: +44 1223 336 033; e-mail: deposit@ccdc.cam.ac.uk).

5. Supporting information

Tables of bond distances and bond angles, atomic coordinates, anisotropic displacement coefficients, hydrogen coordinates, and isotropic displacement parameters for compounds **3** and **4**. Ordering information is given on any current masthead.

Acknowledgements

We thank the FAPESP and the CNPq of Brazil (M.H.A and M.D.V.) and the Ministero della Universitá e della Ricerca Scientifica e Tecnologica of Italy (D.B. and F.G.) for research grants.

References

[1] E. Sappa, A. Tiripicchio, P. Braunstein, Chem. Rev. 83 (1983) 203.

[2] P.R. Raithby, M.J. Rosales, Adv. Inorg. Chem. Radiochem. 29 (1985) 169.

[3] R.L. Mallors, A.J. Blake, P.J. Dyson, B.F.G. Johnson, S. Parsons, Organometallics 16 (1997) 1668.

[4] E. Sappa, J. Cluster Sci. 5 (1994) 211, and references therein.

[5] A.J. Carty, Pure Appl. Chem. 54 (1982) 113.

[6] A. Choualeb, P. Braunstein, J. Rose, R. Welter, Inorg. Chem. 43 (2004) 57.

[7] J.L. Haggitt, B.F.G. Johnson, A.J. Blake, S. Parsons, J. Chem. Soc., Chem. Commun. (1995) 1263.

[8] J.P.H. Charmant, P.J. King, R. Quesada-Pato, E. Sappa, C. Schaefer, J. Chem. Soc., Dalton Trans. (2001) 46.

[9] E. Sappa, O. Gambino, L. Milone, G. Cetini, J. Organomet. Chem. 39 (1972) 169.

[10] A.J. Edwards, N.E. Leadbeater, J. Lewis, P.R. Raithby, J. Chem. Soc., Dalton Trans (1995) 3785.

[11] L.J. Farrugia, N. MacDonald, R.D. Peacock, Polyhedron 17 (1998) 2877.

[12] A.A. Koridze, N.M. Astakhova, F.M. Dolgushin, A.I. Yanovsky, Y.T. Struchkov, P.V. Petrovskii, Organometallics 14 (1995) 2167.

[13] R. Adams, J.E. Babin, M. Tasi, J.-G. Wang, Organometallics 7 (1988) 755.

[14] E. Sappa, A.M.M. Lanfredi, A. Tiripicchio, Inorg. Chim. Acta 42 (1980) 255.

[15] C.-W. Shiu, Y. Chi, C. Chung, S.-M. Peng, G.-H. Lee, Organometallics 17 (1998) 2970, and references therein.

[16] J.P.H. Chartmant, G. Davies, P.L. King, J.R. Wigginton, E. Sappa, Organometallics 19 (2000) 2330.

[17] J.E. Davies, M.J. Mays, P.R. Raithby, K. Sarveswaran, G.A. Solan, J. Chem. Soc., Dalton Trans. (2001) 1269.

[18] E. Delgado, Y. Chi, W. Wang, G. Hogarth, P.J. Low, G.D. Enright, S.-M. Peng, G.-H. Lee, A.J. Carty, Organometallics 17 (1998) 2936.

[19] J. Lunniss, S.A. MacLaughlin, N.J. Taylor, A.J. Carty, E. Sappa, Organometallics 4 (1985) 2066.

[20] E. Sappa, J. Organomet. Chem. 573 (1999) 139.

[21] A.J. Blake, J.L. Haggitt, B.F.G. Johnson, S. Parsons, J. Chem. Soc., Dalton Trans (1997) 991.

[22] P.F. Heveldt, B.F.G. Johnson, J. Lewis, P.R. Raithby, G.M. Sheldrick, J. Chem. Soc., Chem. Commun. (1978) 340.

[23] G.F. Stuntz, J.R. Shapley, C.G. Pierpont, Inorg. Chem. 17 (1978) 2596.

[24] C.G. Pierpont, G.F. Stuntz, J.R. Shapley, J. Am. Chem. Soc. 100 (1978) 616.

[25] A. Ceriotti, R. Della Pergola, F. Demartin, L. Garlaschelli, M. Manassero, N. Masciocchi, Organometallics 11 (1992) 756.

[26] F.S. Livotto, P.R. Raithby, M.D. Vargas, J. Chem. Soc., Dalton Trans. (1993) 1797.

[27] M.H.A. Benvenutti, D. Braga, F. Grepioni, E. Parisini, B.E. Mann, M.D. Vargas, Organometallics 12 (1993) 2955.

[28] D. Braga, F. Grepioni, R.M.S. Pereira, M.D. Vargas, J. Chem. Soc., Chem. Commun. (1993) 1008.

[29] D. Braga, F.Y. Fujiwara, F. Grepioni, R.M.S. Pereira, M.D. Vargas, J. Braz. Chem. Soc. 10 (1999) 35.

[30] R.M.S. Pereira, F.Y. Fujiwara, M.D. Vargas, D. Braga, F. Grepioni, Organometallics 16 (1997) 4833.

[31] M.H.A Benvenutti, P.B. Hitchcock, J.F. Nixon, M.D. Vargas, J. Chem. Soc., Chem. Commun. (1994) 1869.

[32] M.H. Araujo, P.B. Hitchcock, J.F. Nixon, M.D. Vargas, J. Braz. Chem. Soc. 9 (1998) 563.

[33] P.B. Hitchcock, J.F. Nixon, M.D. Vargas, C.M. Ziglio, J. Chem. Soc., Dalton Trans. (2000) 2527.

[34] M.H.A. Benvenutti, D. Braga, F. Grepioni, M.D. Vargas, J. Chem. Soc., Chem. Commun. (1990) 1730.

[35] M.H.A. Benvenutti, D. Braga, F. Grepioni, B.E. Mann, S. Naylor, M.D. Vargas, Organometallics 12 (1993) 2947.

[36] W.B. Fehlammer, H. Stolzenberg, in: G. Wilkinson, F.G.A. Stone, E. Abel (Eds.), Comprehensive Organometallic Chemistry, Pergamon, Oxford, UK, 1982 (Chapter 31.4).

[37] L.A. Brady, A.F. Dyke, S.R. Garner, S.A.R. Knox, S.M. Irving, S.M. Nicholls, A.G. Orpen, J. Chem. Soc., Dalton Trans. (1993) 487.

[38] R.D. Adams, I. Arafa, G. Chen, J.-C. Lii, J.G. Wang, Organometallics 9 (1990) 2350.

[39] G. Ferraris, G. Gervasio, J. Chem. Soc., Dalton Trans. (1973) 1933.

[40] C.G. Pierpont, Inorg. Chem. 16 (1977) 637.

[41] G. Ferraris, G. Gervasio, J. Chem. Soc., Dalton Trans. (1974) 1813.

[42] G. Ferraris, G. Gervasio, J. Chem. Soc., Dalton Trans. (1972) 1057.

[43] A.J. Carty, S.A. MacLaughlin, D. Nucciaroni, Phosphorus 31-NMR Spectroscopy, in: J.G. Verkade, L.D. Quin (Eds.), Stereochemical Analysis of Organic Compounds and Metal Complexes, VCH, Weinheim, 1987 (Chapter 16 and references therein).

[44] C.M. Ziglio, M.D. Vargas, D. Braga, F. Grepioni, J.F. Nixon, J. Organomet. Chem. 656 (2002) 188.

[45] G.M. Sheldrick, SHELX-97, Program for Crystal Structure Determination, University of Göttingen, Göttingen, Germany, 1997.

[46] E. Keller, SCHAKAL99 Graphical Representation of Molecular Models, University of Freiburg, Germany, 1999.